High Strain Rate Deformation Behaviour Analysis of Recycled Aluminium Alloys AA6061 Reinforced Alumina Oxide Al_2O_3 Using Taylor Cylinder Impact Test

*N. Ma'at, C. S. Ho and M. K. Mohd Nor**
Crashworthiness and Collisions Research Group (COLORED),
Advanced Materials and Manufacturing Centre (AMMC),
Faculty of Mechanical and Manufacturing Engineering,
Universiti Tun Hussein Onn Malaysia,
Parit Raja, Batu Pahat, 86400, Johor, Malaysia
**khir@uthm.edu.my*

M. T. Hameed Sultan
Aerospace Manufacturing Research Center (AMRC),
Faculty of Engineering, Universiti Putra Malaysia,
Serdang, 43400 Selangor, Malaysia

ABSTRACT

The deformation behaviour and fracture mechanism of reinforced recycled aluminium alloy are still an open and exciting area to be explored. Based on this motivation, this paper investigates the deformation behaviour, and fracture mode of recycled aluminium alloy AA6061 reinforced alumina oxide at a high strain rate using the Taylor cylinder impact test. The deformation behaviour analysis was also compared with the behaviour shown by the recycled AA6061 without reinforcement material. The geometric profile of the deformed specimen was used to analyse the deformation behaviour and fracture mode, including the relation with the impact deformation characteristics. Three different fracture modes were observed within the impact velocity of 190-370 m/s. The reinforced recycled AA6061 showed a better strength performance with higher critical impact velocity than the unreinforced recycled AA6061. The damage deformation behaviour was studied using Scanning Electron Microscope (SEM). The results showed that the damage agents were initiated, grew, and coalesced during mild ductility

ISSN 1823-5514, eISSN 2550-164X
Received for review: 2022-08-23
Accepted for publication: 2022-10-11
Published: 2022-11-15

https://doi.org/10.24191/jmeche.v11i1.23600

deformation. Damage progression was finally examined using ImageJ software and characterized average voids size. The decrement of voids size was quite significant under tensile splitting and petalling fracture modes compared to the mushrooming due to severe localized plastic strain deformation around this plastic deformation zone. Therefore, the increasing impact velocity increases the severity of damage progression of the reinforced recycled AA6061.

Keywords: *Recycled Aluminium Alloy Reinforced Alumina Oxide; High Velocity Impact Test; Anisotropic Behaviour; Damage Progression; Fracture Mechanism*

Introduction

Aluminium Alloys are one of the most abundant crust elements on the earth, followed by oxygen and silicon. Aluminium Alloys are widely used in many engineering applications such as automotive, aerospace, defense, and others due to their specific strength and excellent mechanical properties. The global demand for aluminium and aluminium products increases because aluminium alloys are lightweight materials with high strength, good thermal conductivity, high corrosion resistance, and low density compared with steel [1]. Aluminium alloy also shows perfect recyclable material where it is the only material that can keep continuously recycled than other common recyclable materials. Producing aluminium alloy from bauxite (ore) is known as primary production while recycling aluminium alloy from waste is known as secondary production. The primary production of aluminium alloy requires high energy consumption (113 GJ/t) while recycling as a secondary option is 90% lower than primary (13.6 GJ/t) [2]. The primary production process also involves the purification of bauxite, the electrolysis process, which consumes electricity, perfluorocarbon (PFC), and CO_2 emissions that lead to environmental pollution due to chemical reactions [1]. Therefore, the studies concluded that recycling aluminium could save energy and cost compared to pure alloy mining from bauxite.

Recycling aluminium has been studied since the 1990s. Numerous recycling approaches have been implemented to serve back to the consumer either for the same application or different. Aluminium alloy is recycled from the first production of an aluminium product were more economical and environmentally friendly than primary production. There are three techniques in the recycling of aluminium alloy that have been studied by many researchers named conventional, semi-direct, and direct recycling. Conventional methods transform aluminium alloy scrap to molten through several manufacturing processes to be used again. The metal is lost during this process. Besides, the conventional method also leads to higher energy consumption and cost and

harms the environment. For the semi-direct method (solid-state), the aluminium alloy scrap turns into new forms by a hot extrusion process or powder metallurgy. However, the direct method turns aluminium alloy chip into a new form without changing its shape by using hot press forging. Direct recycling methods include powder metallurgy [3]-[5], compression [6]-[7], hot extrusion [8]-[9], hot press forging [10], and others. This method is relatively simple, requires less energy, has no effect on the environment, and produces a small amount of waste compared to the conventional method.

The increasing demand and usage of aluminium alloy products worldwide, including the environmental concern, nowadays require the manufacturer to improve, develop an alternative material, and introduce better sustainable material instead of relying on the primary form of aluminium alloy [11]. This issue has attracted the attention of many researchers, designers, and users of aluminium alloys to establish the potential and limitation of such recycled materials depending on the properties and the material response when subjected to extreme loading conditions. Even though secondary aluminium alloy show superior mechanical properties, the failure mode is quite unpredictable and often leads to earlier fracture than its primary form. This situation requires special attention to establish and enhance the material response.

Aluminium Matrix Composite can be regarded as one of the most efficient materials to improve aluminium alloy due to their excellent mechanical properties and fits for numerous applications. The manufacturing process of this composite can be described as a mixing process between the metal with ceramics or plastics as a reinforcement to create superior and unique properties. Aluminium matrix is usually reinforced with hard ceramic such as alumina oxide (Al_2O_3), boron carbide (B_4C), and silica carbide (SiC) which results in high specific modulus, strength, and thermal stability. The aluminium alloy reinforced with boron carbide (B_4C) shows good mechanical and physical properties, but the cost of the raw material is higher [12]. The aluminium alloy reinforced with silica carbide (SiC) has limited structural applications in many engineering situations due to low ductility and fracture toughness [13]-[14]. On the other hand, alumina oxide (Al_2O_3) can improve the mechanical properties of its composite materials compared to the primary nonreinforced alloy.

Many works have been conducted to identify the most reliable recycling process that benefits the environment and economy, finally solving the supply and demand of the primary source of aluminium alloy, including a combination with reinforcement materials [10], [12], [15]-[18]. The findings showed promising performance in terms of the strength of the material, which can be enhanced further using alumina oxide. The study on material response and damage behaviour of recycled aluminium alloys undergoing finite strain deformation also has been considered in a few works; refer to [18]-[19]. It is generally agreed that such recycled material's deformation behaviour and

fracture mode are still an open and exciting area to explore [25]. Therefore, it is crucial to establish the material response before the relevant application can be identified.

In addition, aluminium alloys were anisotropic materials that exhibit different responses for different orientations [17]. Many studies have contributed to the anisotropic influence on material behaviour when subjected to finite strain deformation [17], [18], [26]. The anisotropic deformation of metal is also associated with its mechanical behaviour during forming operations. Anisotropic materials also behave more complicated compared to isotropic materials. This material response complexity is related to the fact that it deforms differently in different directions and orientations, whereas isotropic materials have no preferred orientation [20]. Therefore, it is crucial to examine the influence material response of such material.

In real-life applications, such as automotive and aerospace, the probability of an object colliding with other objects at different impact velocities could arise. Damage and catastrophic failure of the materials could result from the impact [20]. Damage is a series of permanent microstructural changes that modify the thermo-mechanical characteristics. The use of thermo-mechanical loading also forms an arrangement of irreversible physical micro-cracking structures [21]-[22]. The advancement of microstructural highlights in aluminium composites can be used to detect deterioration. The close failure of second-stage particles, incorporations, intermetallic particles, and precipitates is related to the failure procedure in flexible materials.

Taylor Cylinder impact test is an excellent experimental tool for examining material response, fracture mode, and anisotropic behaviour at high strain rates [22]. Rakvåg et al. discovered five unique fracture modes using this experimental approach, as illustrated in Figure 1, including (a) mushrooming, (b) tensile splitting, (c) shear cracking, and (d) petalling, and (e) fragmentation [23]. Impact velocity changes affect deformation and fracture mode [22]-[23]. This test has also been used to examine the behaviour of recycled aluminium alloy [24]-[26]. A non-circular-shaped footprint was observed to indicate anisotropic behaviour and defined the critical impact velocity and fracture mode. It should be noted that this critical value is crucial in the design of any protective structures.

Therefore, the Taylor cylinder impact test was adopted in this work to investigate the material response and fracture mode, including the anisotropic behaviour of recycled aluminium alloy AA6061 reinforced alumina oxide. The results were compared with the hot-forged recycled AA6061 heat-treated to T5-temper [25] to analyse the effect of a reinforcement process on the material characteristics. Generally, the direct recycling process is used to form both recycled materials of a cylindrical shape projectile. The specimen was shot at a (fixed) rigid wall to explore material response under high-strain rate loadings. The cylindrical specimen's post-geometry was investigated in terms of final length, major side profile, and distorted footprint. Microstructural analysis was

performed using Scanning Electron Microscope (SEM) and ImageJ software to check the damage behaviour of the deformed specimen.

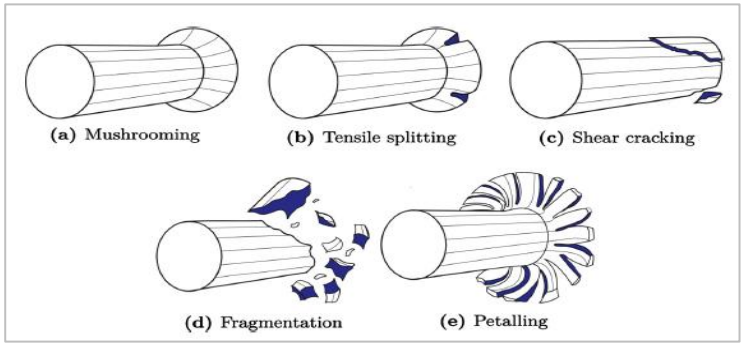

Figure 1: Types of fracture mode [25]

Preliminary Analysis and Taylor Cylinder Impact Test Preparation

Composition and mechanical properties

The chosen material in this paper is the commercial aluminium alloy AA6061, which is commonly utilized in various automotive applications. Table 1 shows the Energy-Dispersive X-ray Spectroscopy (EDS) results of chemical composition comparison between the reinforced recycled AA6061 with the primary AA6061 (primary non-recycled material). The data shows that the reinforced recycled AA6061 has less aluminium(Al)but an equal amount of magnesium (Mg) and silicon (Si) than the primary specimen. In addition, higher carbon (C) and oxygen (O) were obtained primarily due to the formation of severer damage agents such as micro-voids and micro-cracks during the preparation of the specimens. Hence, a noticeable degradation in strength and ductility is expected will be shown by the reinforced recycled AA6061.

The comparison of the mechanical properties of these materials is summarised in Table 2. It should be mentioned that both materials showed strain rate dependency, where the flow stress increases as the strain rate increase. Generally, the reinforced recycled AA6061 shows lower mechanical properties than the primary AA6061. Specifically, Young Modulus, Yield Strength, and Ultimate Tensile Strength (UTS) degraded 0.09%, 14%, and 18.63%, respectively. It can be deduced that the degradation was minimal for the Young Modulus properties within the elastic region. However, a quite pronounced degradation was obtained within the plastic region due to

instability of the reinforcement and grain boundaries of the material to sustain plastic deformation.

Table 1: Chemical composition

Element	Primary AA6061 Atomic (At. %)	Reinforced Recycled AA6061 Atomic (At. %)
Al	89.65	76.64
Mg	0.81	0.81
Si	0.48	0.48
Fe	0.11	0.11
C	5.74	17.74
O	3.21	4.22
Total	100	100

Table 2: Comparison of mechanical properties

Properties	Primary AA6061	Reinforced Recycled AA6061
Young Modulus (GPa)	70.16	63.56
Yield Strength (MPa)	263.67	226.72
UTS (MPa)	312.71	254.44

Projectile preparation

The process to prepare the projectile for analysis using the Taylor Cylinder Impact test is shown in Figure 2. Firstly, the chips are manufactured with an average rectangular shape chip size of 5.2 mm in length, 1.097 mm in width, 0.091 mm thickness as shown in Figure 3 using a MAZAK vertical center Nexus 410A-II- CNC machine with the machining settings provided in Table 3. After that, the chips are cleaned with acetone solution and dried at 60 °C in a thermal oven for around 30 minutes. In this study, the recycled specimens were formed with reinforced material (Alumina Oxide). Then, the chips were mixed with 2.0 wt. % alumina oxide in the SYL 3-dimensional mixer with the speed of 35 r.p.m before the hot press forging recycling process was performed. Subsequently, the chips were poured into the mold. Finally, the recycled specimen was formed using a hot press forging recycling technique with the optimum forming process parameter based on a prior study [10].

The process was carried out at 530°C and 47 MPa (35.6 tonnes) for 2 hours at a constant temperature and pressure. Finally, a wire cut machine was used to shape the recycled specimen into a cylindrical shape with a nominal diameter of 8.45 mm, a length of 15 mm, and a mass of 2.2 g, as illustrated in Figure 4.

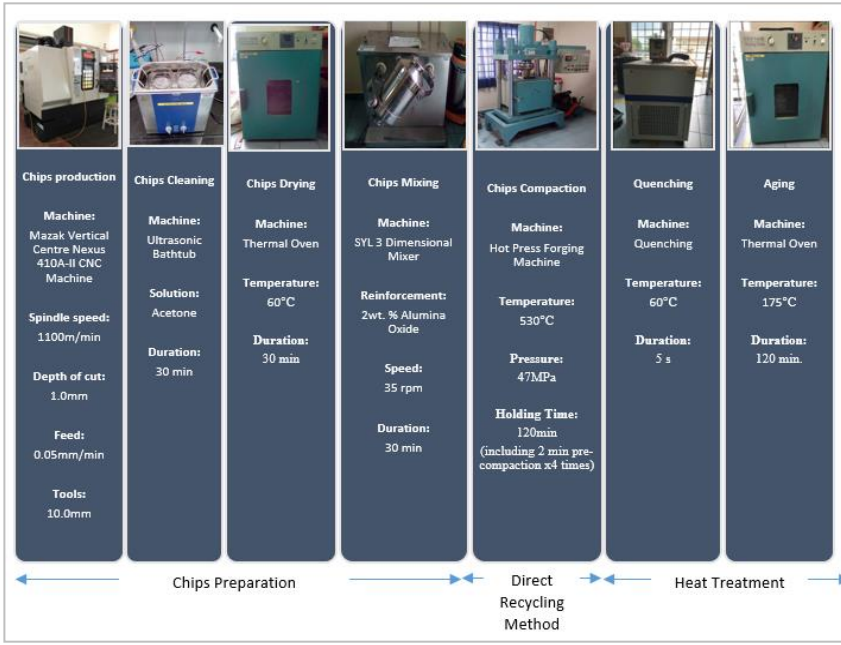

Figure 2: Specimen preparation process of recycled aluminium alloy AA6061 reinforced alumina oxide

Table 3: Setting of recycled chips

Setting	Unit
Speed of Cutting, v	377 m/min
Tool Diameter	10 mm
Feed of teeth, f	0.05 mm/tooth
Depth of Cut	1 mm

Figure 3: Chips geometry

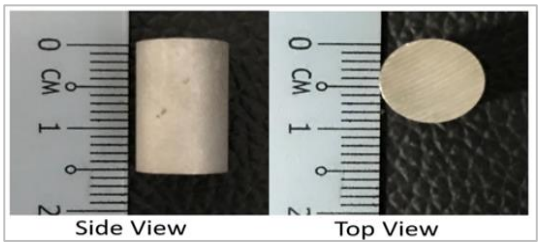

Figure 4: Solid cylindrical shape

Implementation of Taylor cylinder impact test

A schematic diagram of the Taylor cylinder impact experiment is illustrated in Figure 5. This experimental work accelerated the projectiles using a gas gun machine, as shown in Figure 6. First, the specimen was launched at a 150 mm × 150 mm × 10 mm thick fixed target (304 hardened stainless steel block) using pressure as a force. The cylindrical specimen was first placed in the bullet breech. Next, compressed air with a pressure range of 6 to 79 bars was injected into the pressure tank, capable of producing impact velocity ranging from 190 to 370 m/s for a specimen of this weight. Finally, a smooth-bored gun barrel was used to launch the specimen, which exited the barrel and hit the fixed target.

The distance between the tunnel's end and the target was approximately 150 mm, as shown in Figure 7. The specimen's movement within the travel distance was captured using a high-speed camera. Deformation was captured in the 4-microsecond inter-frame of the high-speed camera, which had a resolution time of less than one-tenth of a microsecond (equivalent to 250,000 frames per second).

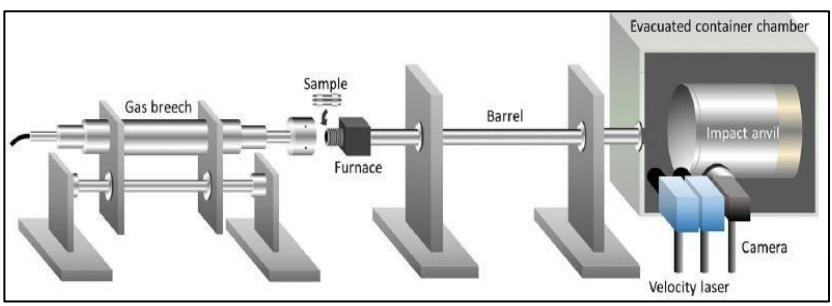

Figure 5: Schematic diagram of Taylor cylinder impact test [20]

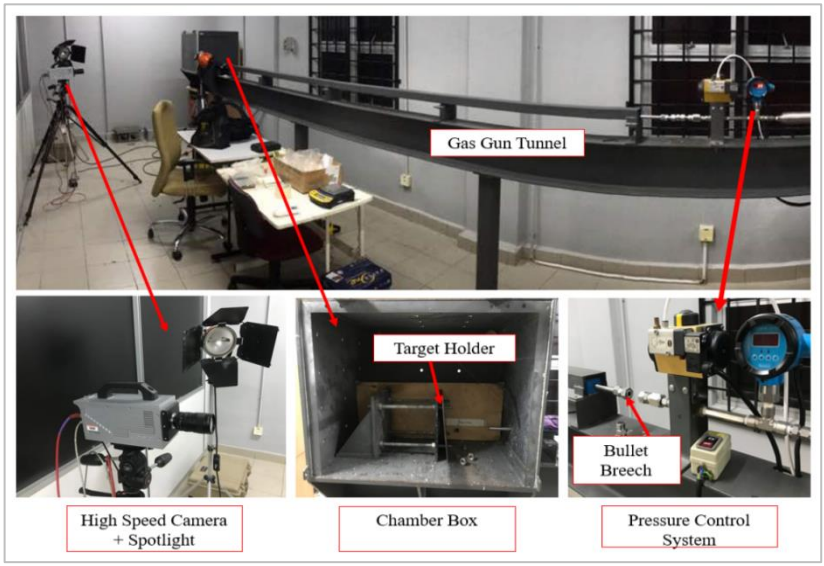

Figure 6: Impact gas gun machine setting

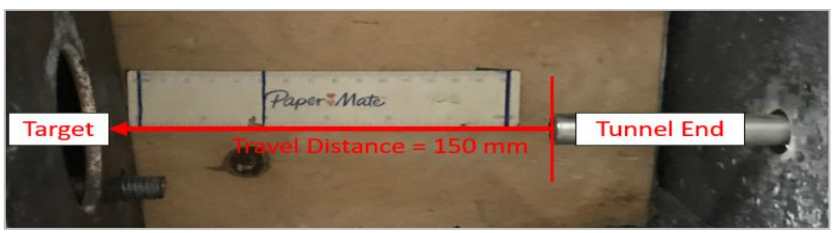

Figure 7: Schematic diagram of impact velocity measurement

Furthermore, the deformed specimens were scanned with a 3D scanner to obtain digitized footprints and geometrical profiles. The specimens' anisotropic behaviour and fracture mode at various impact velocities were examined. Also, critical impact velocity was defined in this analysis, at which deformation occurred before the tensile hoop strained beyond the material's ductility. The damage behaviour of the deformed specimens was examined using SEM before the progression was finally assessed using ImageJ software. To be consistent, the SEM analysis was focused at the center of the sectional cut region, as there might be different fracture deformations, such as petalling and crack, at the edge of the footprint. As aforementioned, the results of each analysis were compared with the recycled AA6061-T5 [25], except for the

damage progression, where the behaviour was characterized in terms of average voids size.

Experimental Result

The impact testing results are discussed in this section. The fracture mode is determined by examining the damage behaviour of the deformed specimens' final length and footprint at various impact velocities. This study also discovered the anisotropic behaviour and the critical impact velocity of the recycled materials.

Fracture mode analysis

The deformed specimen analysis for the reinforced recycled AA6061 at various impact velocities is summarised in Table 4. For comparison, the results of the deformed recycled AA6061-T5 [25] are also listed in the table. Generally, three different fracture modes usually shown by ductile materials can be observed in both specimens: mushrooming, tensile splitting, and petalling. Detail analysis is given in the following sections.

Table 4: Impact behaviour and fracture mode analysis of recycled materials

Specimen	Impact Velocity, V (m/s)	L/D Ratio	Final Length, L_f (mm)	Deformed Length, L_d (mm)	Distance of Major Profile, D_d (mm)	Fracture Mode
Reinforced Recycled AA6061	191	0.826	14.55	7.55	9.94	Mushrooming
	220	0.680	13.05	7.55	10.82	Mushrooming
	231	0.666	12.90	6.80	10.91	Mushrooming
	280	0.620	12.45	6.15	11.31	Tensile Splitting
	322	0.466	11.75	5.25	14.19	Petalling
	358	0.404	10.65	4.9	14.85	Petalling
Recycled AA6061-T5 [25]	195	0.718	13.58	7.54	10.65	Mushrooming
	212	0.742	13.48	7.77	10.24	Mushrooming
	230	0.663	13.13	7.76	11.15	Tensile Splitting
	287	0.545	12.37	7.36	12.79	Tensile Splitting with crack
	328	0.464	11.74	7.06	14.24	Petalling
	367	0.372	10.68	6.72	16.18	Petalling

Mushrooming

Plastic deformation without visible cracks causes mushrooming fracture mode. It occurs when a projectile hits a target at a low velocity, and both elastic and plastic waves are formed at the impact interface immediately after impact. The highest impact velocity observed in this experiment without visible exterior cracks with mushrooming fracture mode was about 231 m/s for the reinforced recycled AA6061 and 212 m/s for recycled AA6061-T5. Photographs of the deformed footprint for the mushrooming fracture mode are shown in Figure 8.

This type of fracture mode can be seen for reinforced recycled specimens at impact velocity ranging from 191 m/s to 231 m/s and recycled AA6061-T5 specimens at impact velocity ranging from 195 m/s to 212 m/s. Again, there were no cracks that could be seen. Figure 9 depicts the matching digitized footprint for mushrooming fracture mode. According to Figure 8, the smallest post-footprint was found at 191 m/s for Reinforced Recycled specimens and 195 m/s for recycled AA6061-T5 specimens at the lowest impact velocity. This condition is due to the impact surface expanding radially during impact deformation due to grain compression in the impact direction.

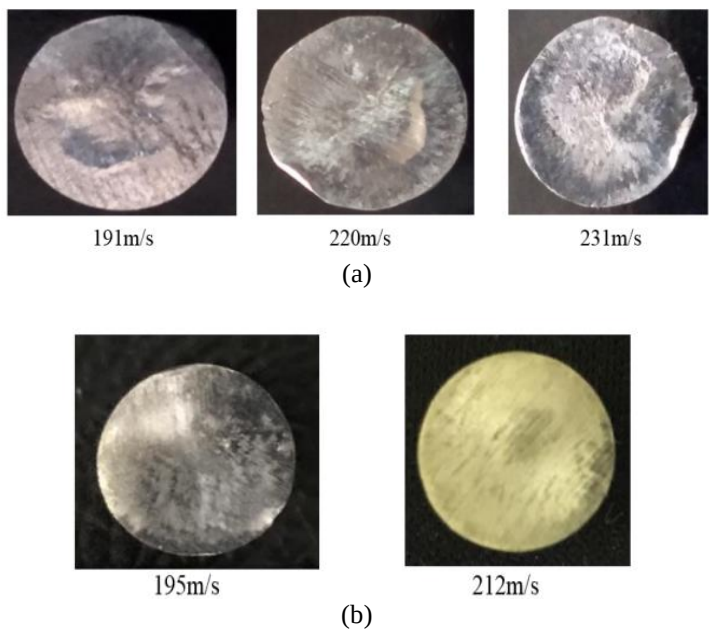

Figure 8: Footprints of the deformed specimens with mushrooming fracture mode; (a) reinforced recycled AA6061, and (b) recycled AA6061 T5 [25]

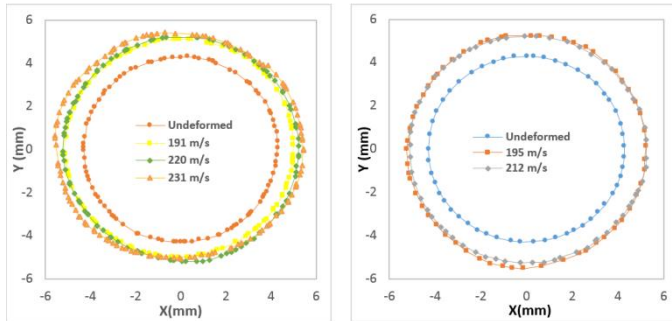

(a) (b)

Figure 9: Digitised locus of the deformed footprints with mushrooming fracture mode; (a) reinforced recycled AA6061, and (b) recycled AA6061-T5 [25]

Tensile splitting

The second fracture mode observed in the reinforced Recycled AA6061 was tensile splitting. Tensile splitting occurred when the specimen was impacted above the critical impact velocity. This fracture mode is observable at an impact velocity of 280 m/s for Reinforced Recycled specimens and from 230 m/s to 287 m/s for recycled AA6061-T5 specimens. The tensile hoop stretching beyond the material's ductility caused this fracture mode. As a result, as seen in Figure 10, cracks can be found at the mushroom end of the deformed footprint.

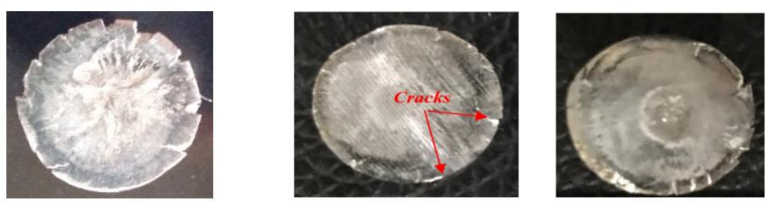

280 m/s 230 m/s 287 m/s

(a) (b)

Figure 10: Photographs of deformed footprint for tensile splitting fracture mode; (a) reinforced recycled AA6061, and (b) recycled AA6061 T5 [25]

The Reinforced recycled specimens demonstrated mushrooming shape at the same impact velocity of 230 m/s, while the recycled AA6061-T5 started deforming in tensile splitting mode. This is an indication of better hardness and ductility at high impact velocity. Therefore, the critical impact velocity for the Reinforced recycled AA6061 and recycled AA6061-T5 can be identified as

higher than 280 m/s and 230 m/s, respectively. As can be noticed, below this critical value, the fracture mode is influenced by plastic deformation represented by a mushrooming shape.

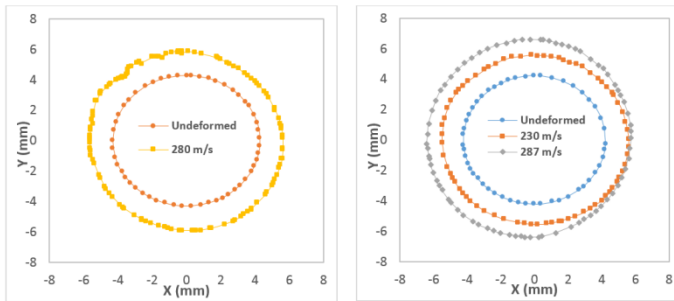

(a) (b)

Figure 11: Digitised locus of deformed specimens with tensile splitting fracture mode; (a) reinforced recycled AA6061, and (b) recycled AA6061-T5 [25]

Petalling

Tensile splitting initiates the petalling fracture mode, transforming into a petalling-shaped (sunflower-like edge) with increasing impact velocity. Both recycled materials experienced petalling fracture mode when impacted from 322 m/s up to a maximum of 367 m/s, as shown in Figure 12. Various visible cracks can be observed as sunflower-like petalling shapes are formed around the edge of the mushrooming footprint. From a comparison of both recycled materials at the same range of impact velocity, it is noticed that the fracture surface looks smooth for the reinforced recycled AA6061 and looks rough with dimples at the central part of the impact surface for the recycled AA6061-T5. The corresponding digitized locus of the deformed specimens is illustrated in Figure 13. The significant circumferential strain formed by the radial motion of the deformation material causes visible cracks and the formation of a sunflower-like edge. Therefore, it could be deduced that this is the most common fracture mode experienced by recycled specimens above their critical impact velocity, as shown by petalling shape, and may lead to a complete fragmentation.

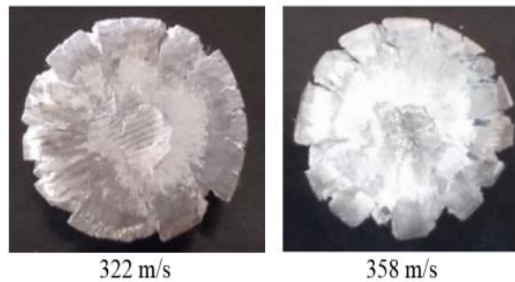

Figure 12: Photographs of deformed footprint for petalling fracture mode; (a) reinforced recycled AA6061, and (b) recycled AA6061 T5 [25]

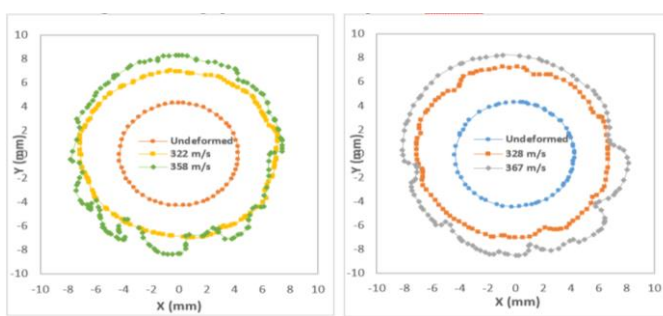

(a) (b)

Figure 13: Digitised locus of deformed specimens with petalling fracture mode; (a) reinforced recycled AA6061, (b) recycled AA6061-T5 [25]

The experiment data shows that the reinforced recycled AA6061 exhibit plastic anisotropic undergoing high-impact velocity deformation similar to the

recycled AA6061-T5. The deformed footprint was distorted in various directions, and the footprint showed a non-symmetric footprint of a non-circular shape. Within the considered impact velocity range, the deformed final length of the specimen decreased from 1 to 4.5 mm from its initial length. The amount of deformation was related to the final length of the specimen. Lower impact velocities (below the critical impact velocity) resulted in fewer deformations, whereas higher impact velocities (above the critical impact velocity) resulted in more localized deformation.

Geometrical shape analysis

Figures 14a and 14b illustrate the post-impact comparison in changes of the length and top diameter of the projectile, respectively. The relationship between these two measurements was also studied in this work. From the observation, with increasing impact velocity, the final length of the projectile was decreased, but increased in the top diameter. Besides, from Figure 13a, at the same velocity impact, the length changes for both materials are almost identical. However, from Figure 13b, around the top diameter of projectiles, the changes experienced by the recycled AA6061-T5 was greater than the reinforced recycled AA6061 projectiles. The reinforced recycled AA6061 projectiles exhibit strong anti-deformation capability compared to recycled AA6061-T5. The reinforcement structures reduce the ability to absorb energy and ductility. This condition is due to hard and brittle alumina, which influence the material's ductility.

Figure 15 shows the relationship between the length to diameter ratio with the impact velocity. Generally, the ratio decreased as the velocity increased for both materials. However, there was a slight increment in the ratio shown by the second impact velocity of the recycled AA6061 - T5. Therefore, it can be concluded that both materials of the projectiles have anti-deformation capabilities.

Metallurgical investigations

The impact surface of the specimens was examined using Scanning Electron Microscope (SEM) to gain a deeper understanding on the deformation behaviour occurring during the impact. Figure 15 represents the SEM micrographs of ×500 magnification scale around the central part of the deformed specimen with mushrooming fracture mode. As can be seen in Figure 15a, irregular shape of fine Al_2O_3 particles are formed in each micrograph around the footprint. This observation was not observed in Figure 15b. This formation gives good effect to the bonding between the particles, hence provide better strength properties compared to recycled AA6061 without reinforced material. From Figure 14, it can be noticed that many dimples, voids and cracks were observed on the impact surface in both recycled materials. It should be noted that damage agents such as micro-cracks and micro-voids are initiated in the pre-test during the specimen formation process. The damage

starts to grow, coalescence and evolve further during the impact deformation and leading to the formation of cracks and large dimples. It can be seen that the damage was less severe in the reinforced recycled AA6061 compared to the recycled AA6061-T5, to withstand higher critical impact velocity.

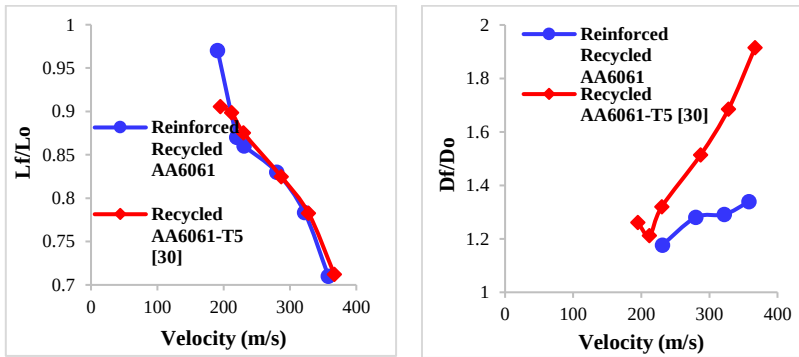

(a) (b)

Figure 14: Comparison changes in length and top diameter of projectiles; (a) residual length vs. impact velocity, and (b) top diameter vs. impact velocity

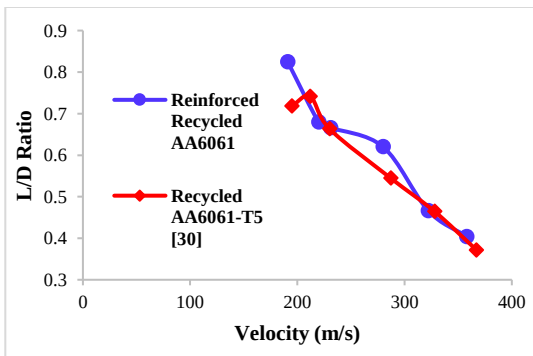

Figure 15: L/D ratio vs. velocity

Further, Figure 17 illustrates the SEM micrographs of the ×500 magnification scale around the central part of the deformed specimens with tensile splitting fracture mode. An apparent damage evolution can be observed as the quantity and size of the cracks and dimples were increased. Voids and dimples grew and coalesced at high speeds, causing the formation of larger dimples and cracks, which finally split at the edge of the footprint. A similar deformation behaviour occurred in the specimen with petalling fracture mode.

The crack lines were obvious and large in the specimen, as shown in Figure 18. The damage coalescence increases with the increase of impact velocity. It can be seen the damage behaviour for the reinforced recycled AA6061 is less severe compared to the recycled AA6061-T5.

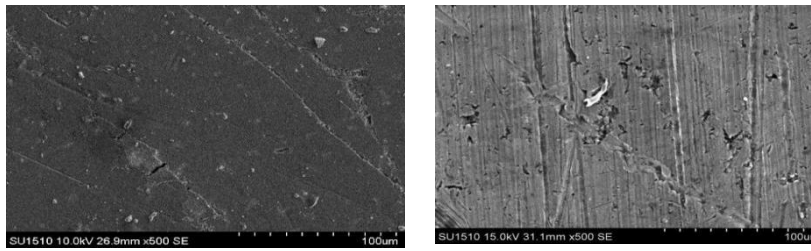

(a) (b)

Figure 16: SEM micrographs of the deformed specimen with mushrooming fracture mode; (a) reinforced recycled AA6061 at 191 m/s, and (b) recycled AA6061-T5 at 195 m/s [25]

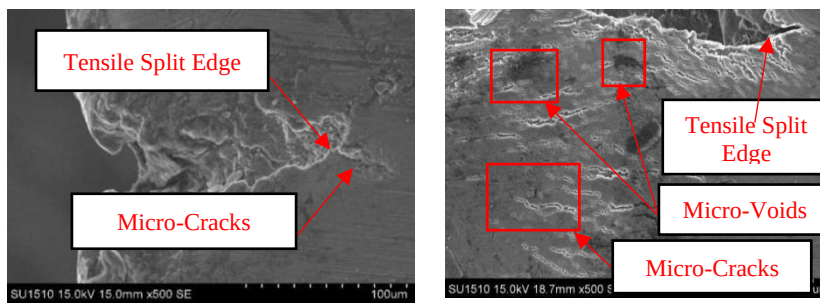

(a) (b)

Figure 17: SEM micrographs in the central part of specimen with tensile splitting fracture mode; (a) reinforced recycled AA6061 at 280m/s, and (b) recycled AA6061-T5 at 287 m/s [25]

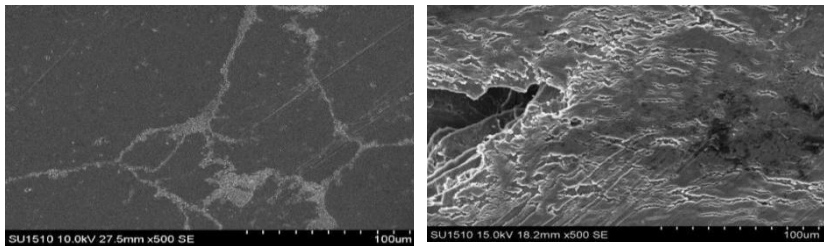

(a) (b)

Figure 18: SEM micrographs in the central part of specimen with petalling fracture mode; (a) reinforced recycled AA6061 at 358m/s, and (b) recycled AA6061-T5 at 367 m/s [25]

Average void size analysis

Focusing only on the reinforced recycled AA6061, the metallurgical investigation was finally used to examine the damage progression of the recycled specimens subjected to impact velocity in terms of average void size. In this analysis, ImageJ software was utilized to measure the numbers of voids around the cross-section located 5 mm above the deformed footprint of the impact surface, where the formation of mushrooming shape ceased in the whole specimens, as schematically shown in Figure 19.

Figure 19: Schematic diagram of the sectional area for damage progression analysis

To prepare for the metallurgical observation around the sectional area, the specimens underwent a grinding process with S_iC paper, polishing with DIAMAT polycrystalline diamond cloths and 0.02 μm SIAMAT non-crystalline colloidal silica, and finally etching with Keller reagents, after being cut with wire cutting, cold-mounted with epoxy resin and hardener. Samples of ImageJ analyses are depicted in Figure 20. Generally, a finer grain matrix is visible within this surface. It should be noted that the analyses were focused right on the center of the deformed surface to avoid inconsistency in the outputs. It was assumed that the shockwave was propagating co-linear to the

impact axis to form a localized plastic strain area at the center point of the surface. This is in line with the observation in the previous analysis where the footprint showed radial expansion to define different fracture modes of the specimens, including cracks around the edge.

Figure 21 shows the results of this analysis. As can be observed the average size of voids decreased as the impact velocity increased. This condition is caused by complex and brittle alumina, which influences the material's ductility and confirms that the damage accumulation is higher for such material. The damage characteristics are directly related to the material's ductility and strength. The smaller the size of micro-voids, the lower the material's ductility and strength [16].

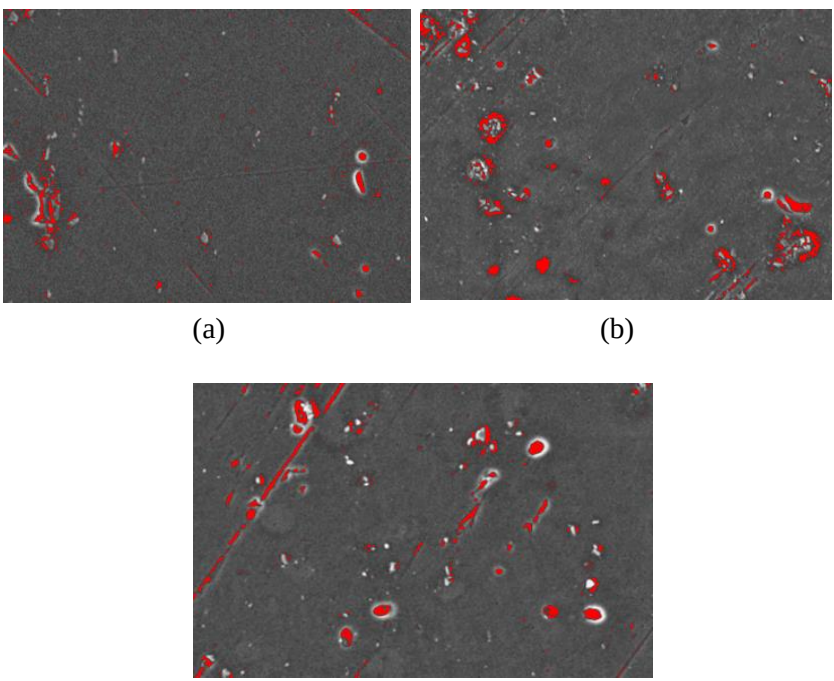

Figure 20: Voids size detection around the sectional surface by ImageJ software: (a) mushrooming, 220 m/s (b) tensile splitting, 280 m/s, and (c) petalling, 322 m/s

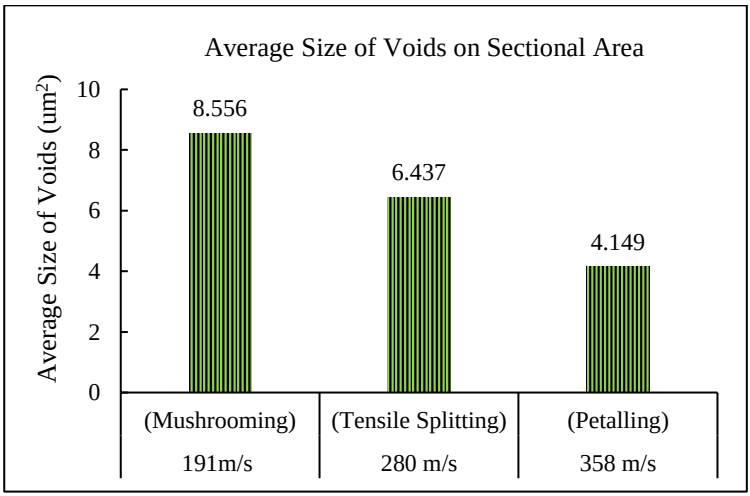

Figure 21: Average size of voids of sectional surface (5 mm above the impact surface)

Conclusion

This paper investigates the deformation behaviour, and fracture modes, including changes in the length and top diameter of the projectile for the recycled aluminium alloy AA6061, reinforced alumina oxide subjected to high-velocity impact, compared with the recycled AA6061-T5. The reinforced recycled AA6061 exhibits better ductility and tensile hoop stress as it can withstand higher critical impact velocity. The critical impact velocity for reinforced recycled AA6061 was lower than 230 m/s. Higher than the critical impact velocity of recycled AA6061-T5 shows that tensile splitting fracture mode with visible cracks was formed at the edge of the footprint when the tensile hoop strained beyond the ductility. The reinforced recycled AA6061 sustained the anisotropic behaviour of its primary source. This can be seen in the deformed footprint's non-circular shape (non-symmetric). Three unique fracture modes are observed within the considered impact velocity: mushrooming, tensile splitting, and petalling. Generally, the deformation behaviour is formed as radial expansion around the impact surface and length reduction. A strain-rate dependency behaviour of such recycled AA6061 was also observed. The reinforced recycled AA6061 projectiles exhibit more vital anti-deformation capability than recycled AA6061-T5 due to complex and brittle alumina, which influenced the material's ductility. From the SEM and ImageJ analyses, it can be noticed that the damage agents, such as cracks and voids, are growing more significantly at higher impact velocity. To conclude,

the recycled AA6061 reinforced Alumina Oxide shows promising strength properties and ductility at a high-velocity impact for a better application identification in various engineering structures.

Acknowledgements

This research was funded by Ministry of Higher Education (MOHE) through Fundamental Research Grant Scheme (FRGS/1/2020/TK02/UTHM/02/5). This research work was also supported by the Aerospace Manufacturing Research Center (AMRC), Faculty of Engineering, Universiti Putra Malaysia, and the Sustainable Manufacturing and Recycling Technology, Advanced Manufacturing and Material Center (SMART AMMC), Faculty of Mechanical and Manufacturing Engineering, Universiti Tun Hussein Onn Malaysia.

References

[1] Y. E. A. Seputra and B. Soegijono and L. Roven, “Engineering of aluminium matrix composite (AMC) reinforcement organoclay based on hotpress method using adaptive neuro-fuzzy inference system (ANFIS)”, *IOP Conference Series: Materials Science and Engineering*, vol. 509, pp. 012156, 2019

[2] N. A. Siddiqui, A. S. Baxtiyarovich, A. Nandan and P. Mondal, “Recent Advances in Recycling Engineering”, *Proceedings of the International Conference on Advances and Innovations in Recycling Engineering*, vol. 25, 2021

[3] M. W. A. Rashid, F. F. Yacob, M. A. Lajis, M. A. Abid, and E. M. T. Ito, "A Review: The Potential of Powder Metallurgy in Recycling Aluminum Chips (Al 6061 & Al 7075)". *In Conference: 24th Design Engineering Systems Division JSME Conference Japan Society of Mechanical Engineers*, pp. 14–27, 2014

[4] M. Rahimian, N. Ehsani, N. Parvin, and H. R. Baharvandi, "The Effect of Particle Size, Sintering Temperature and Sintering Time on the Properties of Al-Al2O3 Composites, Made by Powder Metallurgy”, Journal of Materials Processing Technology, vol. 209, no. 14, pp. 5387–5393, 2009.

[5] M. Rahimian, N. Parvin and N. Ehsani, "The Effect of Production Parameters on Microstructure and Wear Resistance of Powder Metallurgy Al–Al2O3 Composite,” *Materials & Design*, vol. 32, no. 2, pp. 1031–1038, 2011.

[6] B. L. Chan and M. A. Lajis, "Direct Recycling of Aluminium 6061 ChipThrough Cold Compression”, *International Journal of Mechanical & Mechatronics Engineering*, vol. 15, no. 04, pp. 4–8, 2015.

[7] Y. Kume, T. Takahashi, M. Kobashi and N. Kanetake, "Solid State Recycling of Die-cast Aluminum Alloy Chip Wastes by Compressive Torsion Processing", *Journal of Japan Institute of Light Metals*, vol. 59, no. 7, pp. 354–358, 2009.

[8] M. Haase and A. E. Tekkaya, "Recycling of Aluminum Chips by Hot Extrusion with Subsequent Cold Extrusion," *Procedia Engineering*, vol. 81, pp. 652–657, 2014.

[9] A. E. Tekkaya, M. Schikorra, D. Becker, D. Biermann, N. Hammer and K. Pantke, "Hot Profile Extrusion of AA-6060 Aluminum Chips", *Journal of Materials Processing Technology*, vol. 209, no. 7, pp. 3343–3350, 2009.

[10] S. S. Khamis, M. A. Lajis and R. A. O. Albert, "A Sustainable Direct Recycling of Aluminum Chip (AA6061) in Hot Press Forging Employing Response Surface Methodology," *Procedia CIRP*, vol. 26, pp. 477–481, 2015.

[11] G. Gaustad, E. Olivetti, and R. Kirchain, "Improving Aluminum Recycling: A Survey of Sorting and Impurity Removal Technologies". *Resources, Conservation and Recycling*, vol. 58, pp. 79–87, 2012.

[12] B. Chandra and H. Singh, "Science Direct Fabrication and characterisation of Al_2O_3 aluminium alloy 6061 composites fabricated by Stir casting," *Materials Today: Proceedings*, vol. 4, no. 2, pp. 2783–2792, 2017

[13] B. Ravi, B. B. Naik and J. U. Prakash, "Characterization of Aluminium Matrix Composites (AA6061/B4C) Fabricated by Stir Casting Technique," Mater. Today Proc., vol. 2, no. 4–5, pp. 2984–2990, 2015

[14] D. Aruri, K. Adepu and K. Bazavada, "Wear and Mechanical Properties of 6061-T6 Aluminum Alloy Surface Hybrid Composites [(SiC + Gr) and (SiC + Al2O3)] Fabricated by Friction StirPprocessing," J. Mater. Res. Technol., vol. 2, no. 4, pp. 362–369, 2013

[15] C. S. Ho and M. K. Mohd Nor, "Tensile Behaviour and Damage Characteristic of Recycled Aluminium Alloys AA6061 Undergoing Finite Strain Deformation," in Procedding of Institution of Mechanical Engineers, Part C: Journal of Mechanical Engineering Science, 2020

[16] C. S. Ho, M. K. Mohd Nor, N. Ma'at, K. Y. Sim, M. N. Ibrahim, M. A. Lajis and N. K. Yusuf, "Damage Initiation and Evolution Analysis of Hot Extruded Recycled Aluminium Alloys (AA6061)," IOP Conf. Ser. Mater. Sci. Eng., vol. 824, no. 012017, pp. 1–8, 2020

[17] M. K. Mohd Nor, N. Ma'at and C. S. Ho, "Modeling Dynamic Anisotropic Behaviour and Spall Failure in Commercial Aluminium Alloys AA7010. Journal of Dynamic Behavior of Materials, 4, 201-210, 2018

[18] A. Gavrus and H. Francillette, "An Anisotropic Behaviour Analysis of AA2024 Aluminium Alloy Undergoing Large Plastic Deformations," in Aluminium Alloys, Theory and Applications, InTech Open, pp. 49–68, 2011

[19] N. Ma'at, M. K. Mohd Nor, C. S. Ho, N. A. Latif, A. Ismail, K. A. Kamarudin, S. Jamian, M. N. Ibrahim@Tamrin and M. K. Awang, "Effects of Temperatures and Strain Rate on the Mechanical Behaviour of Commercial Aluminium Alloy AA6061", Journal of Advanced Research in Fluid Mechanics and Thermal Sciences, 54(2), 185-190, 2019.

[20] M. K. Mohd Nor, R. Vignjevic and J. Campbell, "Modelling of Shockwave Propagation in Orthotropic Materials," Appl. Mech. Mater., vol. 315, pp. 557–561, 2013

[21] S. Castagne, A. Habraken and S. Cescotto, "Application of a Damage Model to an Aluminium Alloy," J. Damage Mech., vol. 12, no. 1, pp. 5–30, 2003

[22] J. C. Li, G. Chen, F. L. Huang and Y. G. Lu, " Load Characteristics in Taylor Impact Test on Projectiles with Various Nose Shapes," Multidisciplinary Digital Publishing Institute, Metals, 11(5), 713, 2021

[23] Y. Deng, Y. Zhang, X. Xiao and A. Hu " Experimental and numerical study on the ballistic impact behavior of 6061-T651 aluminum alloy thick plates against blunt-nosed projectile," International Journal of Impact Engineering, 144:103659, 2020

[24] E. S. Rodionov, V. G. Lupanov, N. A. Gracheva, P. N. Mayer and A. E. Mayer, " Taylor Impact Tests with Copper Cylinders: Experiments, Microstructural Analysis and 3D SPH Modeling with Dislocation Plasticity and MD-Informed Artificial Neural Network as Equation of State", Multidisciplinary Digital Publishing Institute, Metal, 12, 264, 2022

[25] C. S. Ho, M. A. Rani, M. K. Mohd Nor, N. Ma'at, M. T. H. Sultan, M. A. Lajis and N. K. Yusuf, "Characterization of Anisotropic Damage Behaviour of Recycled Aluminium Alloys AA6061 Undergoing High Velocity Impact," Int. J. Integr. Eng., vol. 11, no. 1, pp. 247–256, 2019

[26] N. Ma'at, M. K. Mohd Nor and C. S. Ho, "Characterisation of Mechanical Properties, Damage Progression and Fracture Modes of Recycled Aluminium Alloy AA6061 Reinforced Alumina Oxide", Internationa Journal of Integrated Engineering, 13(7), 215-255, 2022